

Eigenstate Thermalization Hypothesis (ETH) for off-diagonal matrix elements in integrable spin chains

Federico Rottoli¹ and Vincenzo Alba¹

¹*Dipartimento di Fisica dell'Università di Pisa and INFN Sezione di Pisa,
Largo B. Pontecorvo 3, I-56127 Pisa, Italy.*

We investigate off-diagonal matrix elements of local operators in integrable spin chains, focusing on the isotropic spin-1/2 Heisenberg chain (*XXX* chain). We employ state-of-the-art Algebraic Bethe Ansatz results, which allow us to efficiently compute matrix elements of operators with support up to two sites between generic energy eigenstates. We consider both matrix elements between eigenstates that are in the same thermodynamic macrostate, as well as eigenstates that belong to different macrostates. In the former case, focusing on thermal states we numerically show that matrix elements are compatible with the exponential decay as $\exp(-L|M_{ij}^{\mathcal{O}}|)$. The probability distribution functions of $M_{ij}^{\mathcal{O}}$ depend on the observable and on the macrostate, and are well described by Gumbel distributions. On the other hand, matrix elements between eigenstates in different macrostates decay faster as $\exp(-|M_{ij}^{\mathcal{O}}|L^2)$, with $M_{ij}^{\mathcal{O}}$, again, compatible with a Gumbel distribution.

I. INTRODUCTION

A fundamental problem in the study of out-of-equilibrium quantum many-body physics is to understand how the unitary evolution of isolated systems leads to local equilibration and thermalization. Our current understanding of thermalization is based on the celebrated Eigenstate Thermalization Hypothesis [1–4] (*ETH*). Let H be a generic, i.e., chaotic, many-body Hamiltonian and let $|E_i\rangle$ be its energy eigenstates $H|E_i\rangle = E_i|E_i\rangle$. According to *ETH*, the matrix elements of a generic local operator \mathcal{O} between energy eigenstates take the form [1–4]

$$\langle E_i | \mathcal{O} | E_j \rangle = O(\bar{E}) \delta_{ij} + f_{\mathcal{O}}(\omega, \bar{E}) e^{-S(\bar{E})/2} R_{ij}, \quad (1)$$

where $\bar{E} = \frac{1}{2}(E_i + E_j)$ is the average energy of the eigenstates, $\omega = |E_i - E_j|$, $O(\bar{E})$ is a smooth function of the energy \bar{E} . In (1), $S(\bar{E})$ is the thermodynamic entropy at \bar{E} , $f_{\mathcal{O}}(\omega, \bar{E})$ is a smooth function of its arguments, and R_{ij} is a random variable with mean $\bar{R}_{ij} = 0$ and variance $\bar{R}_{ij}^2 = 1$. Eq. (1) implies that in the thermodynamic limit, since the entropy S is extensive in the system size L , diagonal matrix elements converge to $O(\bar{E})$, i.e., they become smooth functions of the energy *only*. Moreover, the variance of diagonal matrix elements decays exponentially with L . Analogously, off-diagonal matrix elements are exponentially suppressed with increasing L . An intriguing recent result is that the statistics of the off-diagonal matrix elements can be understood in terms of Free Probability Theory [5, 6]. Crucially, Eq. (1) implies local thermalization after quantum quenches in generic, i.e., nonintegrable systems, at least for typical initial states [4]. The *ETH* scaling (1) has been checked numerically for both

diagonal and off-diagonal matrix elements in nonintegrable systems by employing exact diagonalization methods [7–14]. In integrable models, the presence of an extensive number of conserved charges leads to violations of (1), which have been investigated numerically [15–22]. Refs. [23, 24] investigated the *ETH* scaling of diagonal matrix element in *interacting* integrable systems by exploiting Algebraic Bethe Ansatz (*ABA*) results [23, 25] for correlation functions, which allow to reach much larger system sizes compared with exact diagonalization. Precisely, in Ref. [25] showed that the variance of *diagonal* matrix elements decays as L^{-1} , in contrast with (1).

Very recently, Ref. [26] investigated off-diagonal matrix elements of both local and non-local operators in the Lieb-Liniger model, which describes a one-dimensional system of interacting bosons in the continuum. Ref. [26] showed that the finite-size scaling of off-diagonal matrix elements depends crucially on whether $|E_i\rangle$ and $|E_j\rangle$ (cf. (1)) are extracted from the same thermodynamic macrostate, i.e., statical ensemble. Precisely, if $|E_i\rangle, |E_j\rangle$ are in the same macrostate, off-diagonal matrix elements decay exponentially as [26]

$$\langle E_i | \mathcal{O} | E_j \rangle \propto \exp \left[-c^{\mathcal{O}} L \ln(L) - \widetilde{M}_{ij}^{\mathcal{O}} L \right], \quad (2)$$

where $c^{\mathcal{O}} > 0$ is a constant that depends both on the operator \mathcal{O} and on the macrostate. Moreover, the probability distribution function of $\widetilde{M}_{ij}^{\mathcal{O}}$ is well described by a Fréchet distribution. Curiously, the leading term in the large L limit in the exponent of (2) exhibits a logarithmic correction. Notice that the scaling (2) is similar to (1), except for the logarithmic correction and for the non Gaussian

statistics of the $\widetilde{M}_{ij}^{\mathcal{O}}$. The matrix elements of local operators between eigenstates that are in different macrostates exhibit a faster decay in the thermodynamic limit as [26]

$$\langle E_i | \mathcal{O} | E_j \rangle \propto \exp(-d^{\mathcal{O}} L^2), \quad (3)$$

where $d^{\mathcal{O}} > 0$ depends on the macrostates from which $|E_i\rangle$ and $|E_j\rangle$ are extracted and on the operator. Eqs. (2) and (3) were supported by analytic calculations in the hard-core boson limit of the Lieb-Liniger model, and numerical results for the interacting case obtained by exploiting integrability [27, 28].

Although it is natural to expect that the scenario of Ref. [26] applies to generic integrable systems, several aspects deserve further investigation. For instance, Ref. [26] focused on the Lieb-Liniger model, which is a $1D$ quantum field theory model. The question whether the same scenario applies to integrable *lattice* models, such as spin chains, has not been investigated yet. Moreover, Ref. [26] considered the *repulsive* Lieb-Liniger model. Unlike most integrable systems, which possess multi-particle bound states (so-called “strings”) of excitations, the repulsive Lieb-Liniger model features only unbound excitations. Besides being interesting on their own, bound states are also experimentally observable (see Ref. [29] for a recent observation of “strings” in Bose gases). Also, typical equilibrium macrostates, such as thermal states, exhibit a finite density of bound states, implying that bound states are crucial to correctly describe equilibrium and out-of-equilibrium properties. Unfortunately, the presence of bound states renders the computation of matrix elements a daunting challenge. Indeed, despite the fact that exact formulas based on the Algebraic Bethe Ansatz are available for the matrix elements of generic local operators [30, 31], they are plagued by fictitious singularities that have to be regularized to extract numerical results. The presence of bound states significantly increases the complexity of this regularization procedure. Crucially, for operators that have support on a single site the singularities can be removed effectively [32–35], and matrix elements can be obtained with computational cost that grows only polynomially with system size, by exploiting the so-called string hypothesis [36]. Some progress on the numerical computation of diagonal matrix elements of operators acting on more than one site was discussed in Ref. [24]. Precisely, it was shown that for eigenstates that do not contain strings it is possible to numerically construct the reduced density matrix of subsystems of length up to six contiguous sites. This approach was employed in Ref. [25] to

investigate the *ETH* scenario for diagonal operators spin chains.

Here we employ the strategy of Ref. [32] and Ref. [24] to investigate the *ETH* scenario for off-diagonal matrix elements of local operators having support on at most two sites in the spin-1/2 isotropic Heisenberg chain. Following Ref. [26], we focus on eigenstates in the thermal macrostate (Gibbs ensemble). This is a natural choice because thermal states at a given energy density (temperature) are the most abundant ones, the number of non-thermal eigenstates being exponentially suppressed in the thermodynamic limit. We first focus on matrix elements between eigenstates in the same macrostate, considering one-spin operators. We show that off-diagonal matrix elements decay exponentially with L similar to (2). This means that the presence of bound states does not alter the qualitative scenario of Ref. [26]. Next, we consider matrix elements between eigenstates in different macrostates. Precisely, we focus on the zero-temperature and the infinite-temperature macrostates. Similar to (3), off-diagonal matrix elements exhibit the faster decay as e^{-L^2} .

We also numerically extract the probability distribution functions (*PDF*) of M_{ij}

$$M_{ij} = \ln |\langle E_i | \mathcal{O} | E_j \rangle|^2. \quad (4)$$

Quite generically, the *PDFs* are well described by Gumbel distributions, in contrast with Ref. [26]. This confirms the non Gaussian nature of the statistics of off-diagonal matrix element in integrable spin chains. Next, we consider two-spin operators. We focus on thermal macrostates constructed from eigenstates that do not contain strings. In contrast with one-spin operators, for which we can reach $L \sim 500$, for two-spin operators we only provide numerical data for $L \sim 60$. Despite that, our numerical data confirm the scenario observed for one-spin operators.

The manuscript is organized as follows. In Section II we introduce the Heisenberg chain, giving some details on the Bethe Ansatz treatment. In Section II A we introduce the main observables that we consider, the thermodynamic macrostates, and their construction. In Section III we discuss numerical results. We first consider the off-diagonal matrix elements between eigenstates in the same macrostate in Section III A. Specifically, we focus on one-spin operators in Section III A 1, and on two-spin operators in Section III A 2. In Section III A 3 we show that the non Gaussianity of the *PDF* describing off-diagonal matrix elements can be detected from the finite-size behavior of scale-invariant ratios

constructed from (4). This confirms early observations [17]. In Section III B we discuss off-diagonal matrix elements between eigenstates in different macrostates. Finally, we conclude and discuss future directions in Section IV. In Appendix A we provide the *ABA* formulas for the matrix elements of local operators. Precisely, in Appendix A 1 we detail the so-called Slavnov formula for the calculation of scalar products between arbitrary Bethe states. In Appendix A 2 we discuss the formulas for the matrix elements of generic operators (in Appendix A 2 a) and for one-spin operators (in Appendix A 2 b).

II. HEISENBERG SPIN CHAIN

Here we consider the spin-1/2 isotropic Heisenberg chain (*XXX* chain), described by the Hamiltonian

$$H = \frac{J}{4} \sum_{i=1}^L \vec{\sigma}_i \cdot \vec{\sigma}_{i+1}, \quad (5)$$

where $\vec{\sigma}_i = (\sigma_i^x, \sigma_i^y, \sigma_i^z)$ is the vector of Pauli matrices at site i , and L is the length of the system. In the following we set $J = 1$ in (5). The Hamiltonian (5) possesses a $SU(2)$ symmetry generated by the total spin $\vec{S}_T = 1/2 \sum_{i=1}^L \vec{\sigma}_i$, corresponding to global rotations of all the spins. As a consequence, both the total spin \vec{S}_T^2 and the total magnetization along the z direction are good quantum numbers that can be used to label the different eigenstates.

The *XXX* chain Eq. (5) is a paradigmatic example of Bethe Ansatz solvable many-body system [36–39]. In the Bethe ansatz treatment of the *XXX* chain the ferromagnetic state with all the spin up is a “vacuum” state, whereas overturned spins are treated as quasiparticle excitations. Each quasiparticle is labeled by a complex number λ_i , which is called rapidity. Any eigenstate in the sector with fixed number M of quasiparticles, i.e., fixed magnetization, is identified by a set of M rapidities λ_i . The rapidities satisfy nontrivial quantization conditions, encoded in a set of nonlinear coupled algebraic equations as

$$d(\lambda_i) \prod_{j \neq i} \frac{\lambda_j - \lambda_i - i}{\lambda_j - \lambda_i + i} = 1, \quad (6)$$

where the function $d(\lambda)$ is defined as

$$d(\lambda) = \left(\frac{\lambda - \frac{i}{2}}{\lambda + \frac{i}{2}} \right)^L. \quad (7)$$

The Bethe equations (6) admit 2^L sets solutions containing both real and complex rapidities. Complex rapidities correspond to bound states of quasiparticles. Although it is in general challenging to obtain the complex solutions of (6), it was already recognized by Bethe [37] that in the thermodynamic limit $L \rightarrow \infty$ some crucial simplifications occur. Precisely, the vast majority of complex rapidities form “simple” structures in the complex plane known as Bethe strings. Solutions of (6) in the same string have the same real part (string center) and imaginary parts that differ by $\eta = i$. A string of length n corresponds to a bound states of n elementary excitations. In generic integrable systems, strings of arbitrary length are allowed.

Within the framework of the string hypothesis, let us denote the rapidities as $\lambda_{n,\gamma}^j$, with γ labeling the different strings of size n , i.e., that have different string centers, and j labeling the rapidities in the same string. For large L one has for that

$$\lambda_{n,\gamma}^j = \lambda_{n,\gamma} - i(n - 2j - 1) + i\delta_{n,\gamma}^j, \quad (8)$$

where $\delta_{n,\gamma}^j$ are the so-called string deviations, which account for the fact that the string hypothesis holds only in the limit $L \rightarrow \infty$. In (8) $\lambda_{n,\gamma}$ is the string center, and it is real. Real solutions of the Bethe equations correspond to $n = 1$. For the vast majority of the eigenstates of the *XXX* chain string deviations are suppressed exponentially as $\delta_{j,\gamma}^j = \mathcal{O}(e^{-\alpha L})$ (see Ref. [40] for a detailed study of string deviations in the *XXX* chain). In particular, string deviations are not expected to affect the thermodynamic behavior of the model. By employing (8) in Eq. (6), after taking the limit $\delta_{n,\gamma}^j \rightarrow 0$ and considering the logarithm of both members of the Bethe equations, one can write a set of equations for the string centers $\lambda_{n,\gamma}$. One obtains the so-called Bethe-Gaudin-Takahashi equations [36] as

$$L\theta_n(\lambda_{n,\gamma}) = 2\pi I_{n,\gamma} + \sum_{(m,\beta) \neq (n,\gamma)} \Theta_{m,n}(\lambda_{n,\gamma} - \lambda_{m,\beta}), \quad (9)$$

where we defined the scattering phases between different string types $\Theta_{n,m}$ as

$$\Theta_{n,m} = \theta_{|n-m|} + \sum_{r=1}^{(n+m-|n-m|-1)/2} 2\theta_{|n-m|+2r} + \theta_{n+m} \quad (10)$$

for $n \neq m$, and as

$$\Theta_{n,m} = \sum_{r=1}^{n-1} 2\theta_{2r} + \theta_{2n} \quad (11)$$

if $n = m$. In Eqs. (9) to (11) we defined $\theta_n(x) = 2 \arctan(x/n)$. Let us denote by s_n the number of strings of length n in the eigenstate. Thus, one has the total number of particles as $M = \sum_{j=1}^M j s_j$. In (9), $I_{n,\gamma}$ are the Bethe-Gaudin-Takahashi (*BGT*) quantum numbers, and are integer or half-integer numbers for $L - s_n$ odd or even, respectively. For the *XXX* chain the *BGT* quantum numbers satisfy the bound as [36]

$$|I_{n,\gamma}| \leq \frac{1}{2} (L - 1 - \sum_{m=1}^M t_{m,n} s_m), \quad (12)$$

with $t_{m,n} = 2 \min(m, n) - \delta_{n,m}$. In contrast with the Bethe equations (6), the *BGT* equations are much simpler to solve, since their solutions are real.

Moreover, by varying the $I_{n,\gamma}$ allowed by (12), one can target one by one the different solutions, i.e., the different eigenstates of the *XXX* chain. In conclusion, a generic eigenstate of the *XXX* chain is identified by a string configuration $|s_1, s_2, \dots, s_M\rangle$, with s_j the number of strings of length j , and by the associated set of solutions of (9) as

$$|\lambda\rangle = |\{\lambda_{j,\gamma_j}\}_{\gamma_j=1}^{s_j}\}_{j=1,2,\dots,M}, \quad (13)$$

where, again, λ_{j,γ_j} are the string centers for the strings of length j . It is important to stress that since the Hamiltonian (5) commutes with the total spin, its eigenstates are organized into $SU(2)$ multiplets, labeled by the eigenvalue of the total spin S_T^z and the total magnetization S_T^z . Starting from an eigenstate with a given S_T and $S_T^z = S_T$, i.e., with maximum value of the magnetization (highest-weight state), all the descendent eigenstates in the multiplet are obtained by repeated applications of the spin lowering operator $S_T^- = \sum_{j=1}^L S_j^-$, with $S_j^- = (\sigma_j^x - i\sigma_j^y)/2$. One should stress that by solving Eq. (13) for a given M , one obtains only the eigenstates with $S_T^z = S_T$. However, it is well-known [36] that each application of the lowering operator S_T^- corresponds to adding one extra infinite rapidity to the solution of the Bethe equations.

Finally, after solving (9) for the *BGT* rapidities $\lambda_{n,\gamma}$, one can easily obtain the eigenstate expectation value of all the conserved quantities. For instance, the energy reads as

$$E = - \sum_{j,\gamma_j} \frac{2j}{\lambda_{j,\gamma_j}^2 + j^2}. \quad (14)$$

However, here we are interested in matrix elements of local operators, which are not straightforwardly obtained from the solutions of (9). Indeed, the

eigenfunctions of the *XXX* chain, which would allow to compute the matrix elements, contain $\mathcal{O}(2^L)$ components, and are impractical. Moreover, the string hypothesis leads to fictitious singularities in the wavefunction components that have to be carefully removed to extract numerical data. Instead of working with the eigenstates wavefunctions, here we will exploit the fact that exact formulas for the matrix elements have been obtained by using the *ABA* approach [38] (see Section II A).

A. Macrostates and observables

Here we are interested in the statistics of off-diagonal matrix elements of local operators in the thermodynamic limit $L, M \rightarrow \infty$ with M/L fixed. To characterize the thermodynamic behavior of local observables, it is convenient to work with macrostates rather than with individual eigenstates. Macrostates are ensembles of eigenstates that have the same local properties in the thermodynamic limit. Macrostates are identified by the expectation value of *extensive* conserved quantities. For instance, by fixing only the value of the energy density E/L , one obtains the thermal macrostate at a given inverse temperature β . The thermal macrostate describes the “typical” eigenstates at a given energy density. Indeed, although for each value of E/L in the limit $L \rightarrow \infty$ there is an exponentially diverging number of eigenstates that are atypical, i.e., giving nonthermal expectation values for local observables, their fraction is exponentially vanishing compared to the thermal-like eigenstates, which are exponentially more abundant. Notice that the presence of an exponentially diverging number of atypical eigenstates gives rise to nonthermal steady states after quantum quenches in integrable systems, whose description is provided by the Generalized Gibbs Ensemble [41] (*GGE*). On the other hand, for nonintegrable systems atypical eigenstates are expected to be suppressed [15].

Following Ref. [25] and Ref. [26], here we consider matrix elements between eigenstates extracted from thermal macrostates at temperature β . Precisely, we consider the thermal density matrix ρ_{th} defined as

$$\rho_{th}(\beta) = Z^{-1} \sum_{|\lambda\rangle} e^{-\beta E(\lambda)} |\{\lambda\}\rangle \langle \{\lambda\}|, \quad (15)$$

where Z is the partition function. As stressed above, in the thermodynamic limit all the eigenstates in (15) give the same expectation values of

local observables. This is the content of the so-called *weak* Eigenstate Thermalization Hypothesis [15], and it is also at the heart of the Thermodynamic Bethe Ansatz (*TBA*) approach for integrable systems [36]. Now, since the number of eigenstates in (15) grows exponentially with L , and the sum in (15) cannot be performed explicitly, we adopt a sampling strategy, as in Ref. [26] and [25]. Precisely, we employ a Metropolis scheme as in Refs. [25, 42, 43] to sample the eigenstates of the XXX chain with the Gibbs weight $e^{-\beta E}/Z$. Moreover, we restrict ourselves to fixed number of particles, i.e., fixed ratio M/L . We only consider the eigenstates that do not contain infinite rapidities, i.e., eigenstates with largest magnetization (compatibly with M). It is natural to expect that these restrictions do not alter the qualitative scenario, similar to what observed in Ref. [25].

Here we consider local observables that are built from the operators $E_i^{(mn)}$ localized on site i , and defined as

$$\begin{aligned} E_i^{(11)} &= \frac{1}{2}(\mathbb{1}_i + \sigma_i^z), & E_i^{(12)} &= \frac{1}{2}(\sigma_i^x + i\sigma_i^y), \\ E_i^{(21)} &= \frac{1}{2}(\sigma_i^x - i\sigma_i^y), & E_i^{(22)} &= \frac{1}{2}(\mathbb{1}_i - \sigma_i^z). \end{aligned} \quad (16)$$

In the following section, in particular, we will study the statistics of the off-diagonal matrix elements of $E_i^{(11)}$ and $E_i^{(11)}E_{i+1}^{(22)}$, taken as prototypical examples of one and two-spin operators, respectively. The operators (16) are particularly convenient to compute in the XXX model (5), by virtue of the exact results of Refs. [30, 31]. Indeed, a major breakthrough [30, 31] is that it is possible to rewrite the operators (16) in terms of the matrix elements of the so-called transfer matrix of the XXX chain [38], which is at the heart of the *ABA* solution of the model. Then, by using the known action of the transfer matrix on the eigenstates of (5), it is possible to obtain the matrix elements. We review the main results of Refs. [30, 31] in Appendix A, reporting the explicit expression for the matrix elements of the operators in (16). Unlike exact diagonalization approaches, the computational cost to evaluate matrix elements via the *ABA* results reported in appendix A scales exponentially only in the size ℓ of the support of the operator (here we restrict ourselves to $\ell = 1, 2$), but polynomially as $O(M^\ell)$ in the number of particles M . This allows us to reach chain sizes $L \sim 500$ which are prohibitively large for exact diagonalization. Still, we should mention that the numerical implementation of the *ABA* formulas for the matrix elements is nontrivial, because they are derived for an inhomogeneous version of the XXX

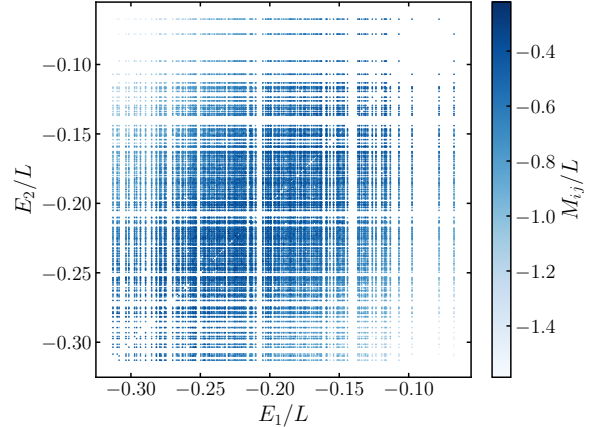


Figure 1. Logarithm of the matrix elements for the one-spin operator $E_j^{(11)}$ with $L = 56$, $M = 14$ as a function of the energy densities E_i/L of the two eigenstates (diagonal elements not reported).

chain. The homogeneous limit that is required to recover (5) introduces fictitious singularities that have to be removed. Furthermore, the presence of string solutions, introduces additional singularities, which have to be dealt with by carefully taking the limit of vanishing string deviations. For the operators with support on more than one site, treating the homogeneous limit and the limit of vanishing string deviations at the same time is very challenging. For this reason, as in Ref. [24], we only consider off-diagonal matrix elements of $E_i^{(11)}E_{i+1}^{(22)}$ between eigenstates without bound states. For one-spin operators, since the homogeneous limit is trivial, the limit of vanishing string deviations can be performed analytically. Thus, for one-spin operators we are able to investigate the effect of bound states on the finite-size scaling of matrix elements.

III. NUMERICAL RESULTS

Before discussing our main results, let us discuss some qualitative features of off-diagonal matrix elements. First, given the operator \mathcal{O} of interest, let us define the main quantity of interest M_{ij} as

$$M_{ij} = \ln |\langle E_i | \mathcal{O} | E_j \rangle|^2 = \ln |\mathcal{O}_{ij}|^2. \quad (17)$$

In Fig. 1 we overview the behavior of M_{ij} for the one-spin operator $E_i^{(11)}$ (cf. (16)) in the XXX chain with $L = 56$, $M = L/4$. The data shown in the figure are for the infinite-temperature macrostate. Precisely, by employing the method of Ref. [42]

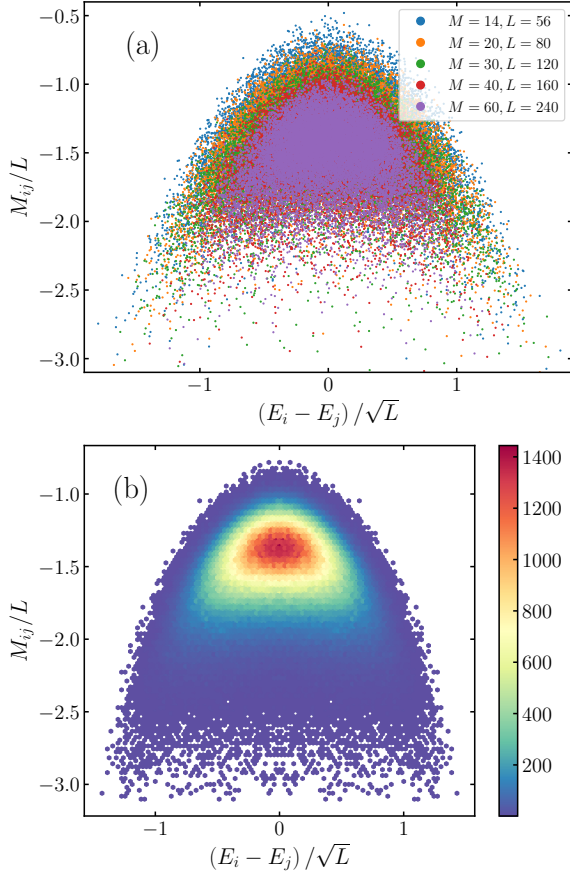


Figure 2. Scaling of the logarithm M_{ij} (cf. Eq. (17)) of the matrix elements of the one-spin operator $E_i^{(11)}$ as a function of $E_i - E_j$, with E_i, E_j the energy of the two eigenstates. (a) Scatter plot of the logarithm M_{ij} rescaled by L as a function of $(E_i - E_j)/\sqrt{L}$ for $L = 56, 80, 120, 160$, and 240 and fixed $M = L/4$. (b) Two-dimensional histogram of the rescaled logarithm M_{ij}/L as a function of $(E_i - E_j)/\sqrt{L}$.

we generate an ensemble of $\sim 10^3$ eigenstates of the XX chain distributed with the infinite-temperature Gibbs probability. As discussed earlier, we fix the magnetization $M/L = 1/4$ and consider only the eigenstates that correspond to solutions of the Bethe equations without infinite rapidities. On the two axes we show the energy density E_1/L and E_2/L of the eigenstates. Here we have $E_1/L, E_2/L \in [-0.3, -0.1]$. Notice that in the thermodynamic limit $L, M \rightarrow \infty$, the fluctuations of the energy density are suppressed as $1/\sqrt{L}$, i.e., the energy density peaks at the thermal value at the density $M/L = 1/4$. Again, this reflects that in the thermodynamic limit all the eigenstates in the thermal ensemble give the same expectation

value for local observables. The dots in the plot are the values of M_{ij}/L , the color intensity being their magnitude. We omit the diagonal matrix elements. The smallest off-diagonal matrix elements are $\approx 10^{-25} \sim e^{-L}$.

It is interesting to investigate the dependence of M_{ij} on the energy difference $E_i - E_j$. This is illustrated in Fig. 2 (a) plotting M_{ij}/L versus $(E_i - E_j)/\sqrt{L}$, where the $1/\sqrt{L}$ accounts for the fact that in the thermodynamic limit the energy peaks around its thermal value with \sqrt{L} fluctuations. The different colors now correspond to different chain sizes $L \leq 240$, with fixed particle density $M/L = 1/4$. The data for different L overlap in the large L limit, suggesting that $M_{ij} \sim L$. The largest off-diagonal matrix elements M_{ij} occur for $E_j = E_i$, and M_{ij} increases if the eigenstates are farther apart in energy. In Fig. 2 (b) we report with the color scale the number of matrix elements. Clearly, the most abundant values of M_{ij} are at $E_i - E_j \approx 0$ and peak around $M_{ij}/L \approx -1.5$.

A. Statistics of matrix elements between eigenstates in the same macrostate

Here we quantitatively address the finite-size scaling of off-diagonal matrix elements and their statistics. Precisely, we consider both one-spin and two-spin operators in Section III A 1 and Section III A 2, respectively. Finally, in Section III A 3 we show that the non Gaussianity of the probability distribution of off-diagonal matrix elements is reflected in the divergence with L of an ad hoc defined ratio of matrix elements.

1. One-spin operator

In Fig. 3 we report M_{ij} (cf. (17)) for the operator $E_i^{(11)}$ (cf. (16)). In Fig. 3 (a) we show the histograms $P(|M_{ij}|)$ for several chain sizes up to $L = 240$, at fixed particle density $M/L = 1/4$. The data are the same as in Fig. 2 (b) for the infinite-temperature macrostate. We observe that as L increases, the center of the peak moves towards larger values of $|M_{ij}|$, and the distribution broadens. Moreover, the histograms are not symmetric around the maximum, suggesting non Gaussian behavior. Notice that at $L = 240$ the typical off-diagonal matrix elements is $M_{ij} \sim 10^{-200}$. Indeed, to correctly capture such tiny matrix elements we employed arbitrary-precision arithmetic in evaluating the ABA formulas (see Appendix A). Let us now discuss the statistics

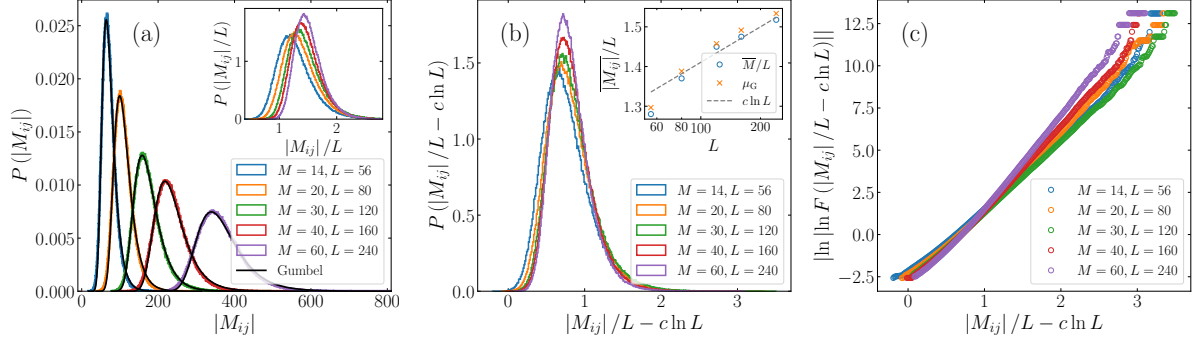


Figure 3. Distribution of the logarithm $|M_{ij}|$ (cf. (17)) of the matrix elements of the one-spin operator $E_i^{(11)}$ (cf. (16)) for eigenstates of the XXX chain with particle number $M = 14, 20, 30, 40$, and 60 and chain size $L = 4M$. Eigenstates are extracted from the infinite-temperature thermal macrostate. (a) Histogram of $|M_{ij}|$. The continuous lines are fits to the Gumbel distribution (19), with β, μ fitting parameters. In the inset we report the histogram of $|M_{ij}|/L$. (b) Histograms of the shifted $|M_{ij}|/L - c \ln L$, with c a parameter obtained by fitting the average $\overline{|M_{ij}|}/L$ to the behavior $c \ln L + c_0$, with c_0 another fitting parameter. The fit is reported as gray-dashed line in the inset. In the inset μ_G is the mean of the Gumbel distribution, i.e., $\mu_G = \mu + \beta\gamma$, with β, μ as in (19) and γ the Euler-Mascheroni constant. To compute μ_G we used the fitted values of β, μ in panel (a). (c) Double logarithm of the cumulative distribution function (CDF) $F(|M_{ij}|/L - c \ln L)$ as extracted from the numerical data.

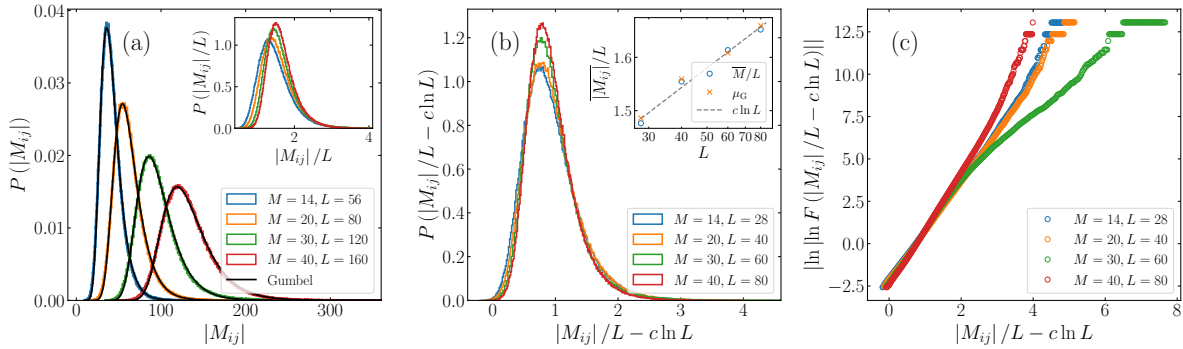


Figure 4. Same analysis as in Fig. 3 for eigenstates of the XXX chain in the infinite-temperature macrostate with particle density $M/L = 1/2$.

of the off-diagonal matrix elements, i.e., the functional form of the distribution $P(M_{ij})$. For the Lieb-Liniger gas, Ref. [26] showed that $P(|M_{ij}|/L)$ is well described by a Fréchet distribution $P_{\alpha, \beta, \nu}$, whose probability distribution function takes the form

$$P_{\alpha, \beta, \nu}(x) = (x - \nu)^{-\alpha-1} \exp \left[- \left(\frac{x - \nu}{\beta} \right)^{-\alpha} \right], \quad (18)$$

for $x > \nu$, and it is zero otherwise. By fitting the data in Fig. 3 to (18), we obtain $\beta \approx -\nu$ and quite large values of $\beta \sim 10^3$. In the limit of large $\beta = -\nu$ the Fréchet distribution reduces to the Gumbel distribution $P_{\mu, \beta}$ given by

$$P_{\mu, \beta}(x) = \frac{1}{\beta} e^{-\frac{x-\mu}{\beta}} - e^{-\frac{x-\mu}{\beta}}, \quad (19)$$

The continuous lines in Fig. 3 are fits to (19) with β, μ the fitting parameters. For all the values of L the data are quite well described by (19). To proceed, we observe that according to ETH (cf. (1)), one should expect that $M_{ij} \sim -L$, which has been verified in Ref. [26] for the Lieb-Liniger model. Thus, in the inset of Fig. 3 we report the histograms $P(M_{ij}/L)$. The collapse of the data for different L is not perfect, as a residual “drift” towards the right is visible. This is expected, and it was observed also for the Lieb-Liniger gas [26]. This effect can be fully accounted for by a residual L dependence of the parameter μ of the distribution, which is related to the average of the Gumbel distribution $\mu_G = \mu + \beta\gamma$, with γ the Euler-Mascheroni constant. Thus, let us consider the average $\overline{M_{ij}}$ as a

function of L . Following Ref. [26] we fit \overline{M}_{ij}/L to the behavior

$$\overline{M}_{ij} = -cL \ln(L) - c_0 L, \quad (20)$$

with c, c_0 fitting parameters. By fitting the data with $L \geq 80$ we obtain $c \approx 0.13$ and $c_0 \approx 0.82$. Now, the histograms of $|M_{ij}| - c \ln(L)$ for different values of L should collapse on the same curve, at least in the limit $L \rightarrow \infty$. In Fig. 3 (b) we show the distribution of $|M_{ij}|/L - c \ln(L)$, with c the fitted value. The data collapse for different L improves as compared with Fig. 3 (a), although it is not perfect. This could be attributed to residual finite L corrections. In the inset of Fig. 3 (b) we report $|\overline{M}_{ij}|/L$ versus L (notice the logarithmic scale on the x -axis). The dashed line is the fit to (20). The crosses denote the average of the Gumbel distribution μ_G computed from the fitted constants μ, β extracted in panel (a), and are compatible with \overline{M}_{ij}/L . It is also interesting to consider the Cumulative Distribution Function (*CDF*) $F(x)$ of the Gumbel distribution is

$$F(x) = \int_{-\infty}^x P_{\mu, \beta}(t) dt = e^{-e^{-\frac{x-\mu}{\beta}}}. \quad (21)$$

Eq. (21) implies that the double logarithm of $F(x)$ is a straight line. In Fig. 3 (c) we show the double logarithm of the *CDF* of $|M_{ij}|/L - c \ln(L)$ as extracted from the numerical data. The data exhibits an approximate linear behavior as a function $|M_{ij}|/L - c \ln(L)$ in the central region, whereas deviations from linear scaling are visible at the edges, which correspond to the tails of the distribution, where finite L effects are expected to be larger.

An important question is how universal is the statistics of off-diagonal matrix elements. To investigate this aspect, we consider the infinite-temperature thermal ensemble at fixed particle density $M/L = 1/2$. Numerical data are reported in Fig. 4. The qualitative behavior is similar to that at $M/L = 1/4$ (see Fig. 3). The continuous lines in Fig. 4 (a) are fits to the Gumbel distribution (19), and are in good agreement with the numerical data. In the inset of Fig. 4 (a) we report the rescaled histograms of $|M_{ij}|/L$. The collapse is not perfect, similar to the case with $M/L = 1/4$. We employ the same strategy as for $M/L = 1/4$, i.e., fitting the average \overline{M}_{ij}/L to (20), and plotting in Fig. 4 the shifted $M_{ij}/L - c \ln(L)$. The fit to the expected scaling (20) gives $c \approx 0.16, c_0 \approx 0.94$ (see the inset in panel (b)). It is clear that the probability distribution $P(M_{ij} - c \ln(L))$ is different than that for $M/L = 1/4$. The data collapse for different

L is better than for $M/L = 1/4$, and deviations near the peak become smaller upon increasing L . A fit of the histogram for $L = 80$ to the Gumbel (19) gives $\beta \approx 0.29, \mu \approx 0.77$. Finally, in Fig. 4 (c) we report the double logarithm of the numerical *CDF* for $|M_{ij}|/L - c \ln(L)$. As for $M = 1/4$, in the central region the *CDF* exhibits a clear linear behavior, as expected.

2. Two-spin operator

Let us now discuss the statistics of off-diagonal matrix elements of local operators that have support on two nearest-neighbor sites. In the following we consider the infinite-temperature macrostate at $M/L = 1/4$. Moreover, since we employ the approach of Ref. [25], as stressed already we are restricted to the macrostate constructed from eigenstates of the *XXX* chain that do not contain bound states. Moreover, since the computational cost for evaluating the *ABA* formulas (see appendix A) increases exponentially with the size of the operator support, we provide results for $L \leq 60$. We anticipate that, despite this limitations, the qualitative scenario outlined for the one-spin operators remains the same. Let us focus on the operator $E_i^{(11)} E_{i+1}^{(22)} = (\mathbb{1}_i - \sigma_i^z)(\mathbb{1}_{i+1} + \sigma_{i+1}^z)/4$, which is sensitive to anti-aligned spin configurations on nearest-neighbor sites.

In Fig. 5 (a) we report the histogram of M_{ij} . The continuous lines are fits to the Gumbel distributions (19), which are in perfect agreement with the numerical data. In Fig. 5 (b) we show the histograms of the shifted $\overline{M}_{ij} - c \ln(L)$, with c obtained by fitting the average \overline{M}_{ij}/L to (20) (see the inset in panel (b)). The fit gives $c \approx 0.25, c_0 \approx 0.15$. Despite the smaller chain sizes as compared with Figs. 3 and 4, the data exhibit a reasonable collapse. A fit to the Gumbel distribution (19) gives $\beta \approx 0.28, \mu \approx 0$. Finally, in Fig. 5 (c) we plot the double logarithm of the *CDF* of \overline{M}_{ij} . Again, the approximate linear behavior in the central region confirms that M_{ij} are well described by the Gumbel distribution.

3. Non-Gaussianity of off-diagonal matrix elements

Our results for off-diagonal matrix elements confirm that, despite integrability, the finite-size scaling is similar to the *ETH* scaling (1), even quantitatively. Precisely, the exponential decay as e^{-L} is

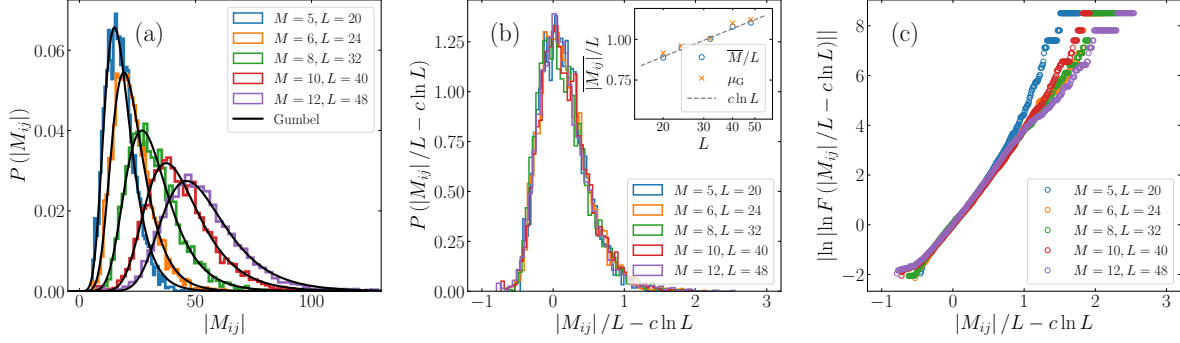


Figure 5. Distribution of M_{ij} in Eq. (17) of the two-spin operator $E_i^{(11)}E_{i+1}^{(22)}$ for $L = 20, 24, 32, 40$, and 48 and $M = L/4$. (a) Histogram of the absolute value $|M_{ij}|$. The continuous lines are fits to the Gumbel distribution (19), with μ, β fitting parameters. (b) Histograms of $|M_{ij}|/L - c \ln(L)$, with c obtained by fitting the average \bar{M}_{ij}/L to the expected scaling (20). The fit is reported in the inset with the gray-dashed line. We report with the cross symbols the average of the Gumbel distributions $\mu_G = \mu + \beta\gamma$, with μ, β obtained from the fits in panel (a), and γ the Euler-Mascheroni constant. (c) Double logarithm of the CDF of $|M_{ij}|/L - c \ln(L)$.

the same, except for the correction (20). The difference between integrable and non-integrable models emerges strikingly in the statistics of M_{ij} . According to the ETH (1), in chaotic models R_{ij} follow a Gaussian distribution with zero mean and variance that depends on the energies E_i and E_j of the two eigenstates. On the other hand, we showed that in integrable systems M_{ij} is well described by a Gumbel distribution.

To investigate the effects of the non Gaussianity of M_{ij} , following Ref. [17], we compute the ratio Γ defined as

$$\Gamma = \frac{\overline{|\mathcal{O}_{ij}|^2}}{\overline{|\mathcal{O}_{ij}|}^2}. \quad (22)$$

Here \mathcal{O}_{ij} is the matrix element between the eigenstates with energy E_i and E_j , and $\overline{|\mathcal{O}_{ij}|^2}$ and $\overline{|\mathcal{O}_{ij}|}$ are the averages of $|\mathcal{O}_{ij}|^2$ and $|\mathcal{O}_{ij}|$ calculated over all the eigenstates with energies E_i and E_j such that $|E_i - E_j| \leq \Delta E$. Here we choose the energy window $\Delta E = 1.25$. For zero-mean Gaussian distributed \mathcal{O}_{ij} , the ratio Γ is equal to $\pi/2$, and it is independent of the variance. This has been verified by using exact diagonalization in several nonintegrable systems (see, for instance, Ref. [17]).

In Fig. 6 we plot the ratio (22) as a function of the energy difference $(E_i - E_j)/\sqrt{L}$. In the main plot, we consider the matrix elements \mathcal{O}_{ij} of the one-spin operator $E_i^{(11)}$, whereas in the inset those of the two-spin one $E_i^{(1,1)}E_{i+1}^{(2,2)}$ (cf. (16)). Clearly, Γ differs significantly from $\pi/2$, for both operators. Actually, we observe $\Gamma \sim 10^5$ in the region with $E_i \approx E_j$. We should mention that while the finite-

size scaling of Γ in the Heisenberg chain was already investigated in Ref. [17] by employing exact diagonalization, here we provide numerical data for much larger size $L \leq 240$. The fact that $\Gamma \sim 10^5$ suggests that Γ diverges in the thermodynamic limit $L \rightarrow \infty$. Indeed, we observe that Γ grows upon increasing the total number of off-diagonal matrix elements employed to compute (22). This is compatible with the fact that \bar{M}_{ij} is well described by a Gumbel distribution, as we now show. First, we can neglect the logarithmic correction (20) because it depends weakly on $|\mathcal{O}_{ij}|$ and it cancels out in the ratio (22). A straightforward calculation allows us to obtain from (19) the distribution of $|\mathcal{O}_{ij}|$ as

$$P(y) = \frac{1}{\beta L y} e^{-e^{\mu/\beta} y^{1/(\beta L)}} e^{\mu/\beta} y^{1/(\beta L)}. \quad (23)$$

Now, one can compute Γ in (22). Clearly, one obtains that both the numerator and the denominator in (22) vanish in the limit $L \rightarrow \infty$. However, one can check that the ratio Γ diverges exponentially in the limit $L \rightarrow \infty$, consistent with the observation in Fig. 6.

B. Statistics of matrix elements between eigenstates involving different macrostates

Let us now discuss off-diagonal matrix elements between eigenstates that are in different thermodynamic macrostates. First, exact results for hard-core bosons and numerical ones for the Lieb-Liniger gas (see [26]) suggest that off-diagonal matrix elements

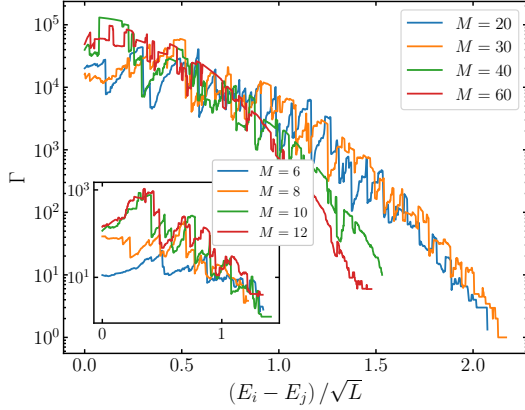


Figure 6. Value of the ratio Γ in Eq. (22) for the operator $E_i^{(11)}$ for $M = 20, 30, 40$, (cf. (16)) and 60 and $L = 4M$ (main plot). In the inset we show the ratio Γ for the two-spin operator $E_i^{(11)} E_{i+1}^{(22)}$.

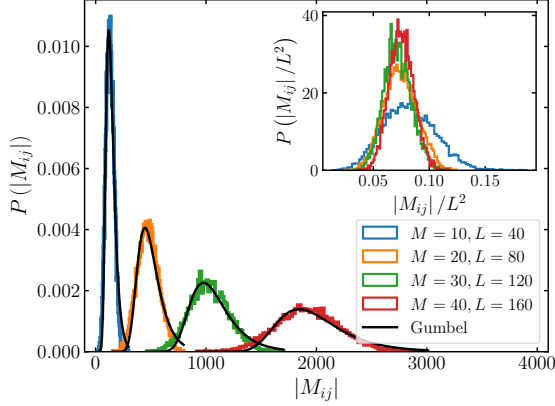


Figure 7. Distribution of the logarithm of the matrix element $|M_{ij}|$ of the one-spin operator $E_i^{(11)}$ between eigenstates in different macrostates. In the inset we report the histogram of $|M_{ij}|$ rescaled with L^2 . The data for $L = 120$ and 160 collapse on the same curve.

decay as

$$\langle E_i | \mathcal{O} | E_j \rangle \sim \exp(-M'_{ij} \circ L^2), \quad (24)$$

where $M'_{ij} \circ$ depends on the observable and on the two macrostates. Here we focus on the infinite-temperature and the zero-temperature (i.e., the ground state) macrostates. Indeed, we numerically observe that it is in general challenging to reach the asymptotic regime $L \rightarrow \infty$, where (3) is expected to hold. This could be attributed to the eigenstates-to-eigenstates fluctuations within the same macrostate at finite size L . These fluctuations give rise to “overlaps” between the two macrostates,

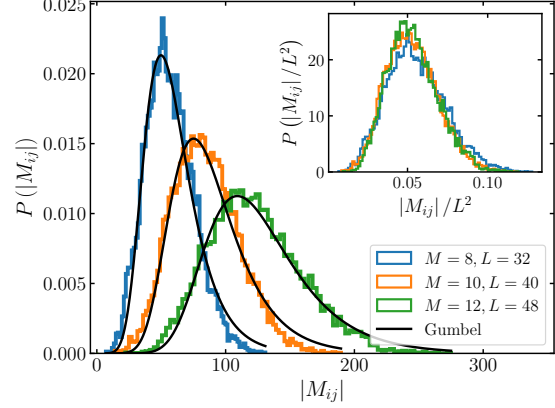


Figure 8. Distribution of the logarithm of the matrix element $|M_{ij}|$ of the two-spin operator $E_i^{(11)} E_{i+1}^{(22)}$ between eigenstates in different macrostates, for $L = 32, 40$, and 48 and $M = L/4$. In the main plot we report the histogram of the absolute value of $|M_{ij}|$. In the inset we plot the logarithm $|M_{ij}|$ rescaled by L^2 , observing a collapse.

which make challenging to observe the asymptotic scaling (24). It is natural to expect that the choice of the macrostates with $\beta = 0$ and $\beta = \infty$ is expected to minimize such finite-size corrections.

In Fig. 7 we show the histograms of the off-diagonal matrix elements $M_{ij} = \ln(|\langle E_i | \mathcal{O} | E_j \rangle|^2)$ for the one-spin operator $E_i^{(11)}$ (cf. (16)). As in Section III A, we show results for $L = 40, 80, 120$, and 160 and fixed particle density $M = L/4$. By comparing with Fig. 3 (a) we observe that the typical value of $M_{ij} \approx 10^3$ is much larger than for off-diagonal matrix elements between eigenstates in the same macrostate, which is compatible with the faster exponential decay Eq. (3). To extract the probability distribution function of M_{ij} , we fit the data to the Gumbel distribution (19). The fits are reported with the continuous lines. The agreement between the data and the fits is not as good as for matrix elements between eigenstates in the same macrostate, although this could be a finite L effect. To test the expected scaling (3), in the inset of Fig. 7 we plot $|M_{ij}|/L^2$. The figure shows that all the data for $L \geq 80$ collapse on the same curve. In Fig. 8 we perform a similar analysis for the two-spin operator $E_i^{(11)} E_{i+1}^{(22)}$, showing data for $L = 32, 40$, and 48 and $M = L/4$. Again, the qualitative behavior of the data is similar as in Fig. 7, in agreement with Eq. (3).

IV. CONCLUSIONS

We investigated the *ETH* scenario for off-diagonal matrix elements in the $\frac{1}{2}$ -spin *XXX* chain, which is a paradigmatic example of integrable lattice many-body quantum system. By employing state-of-the-art Algebraic Bethe Ansatz formulas, we studied off-diagonal matrix elements involving one-spin and two-spin operators up to chain sizes $L \leq 240$, which are far beyond state-of-the-art exact diagonalization results. We focused on the statistics of off-diagonal matrix elements between eigenstates that are both in the same thermodynamic macrostate, as well as eigenstates in different macrostates. Our results confirm the finite-size scaling observed in 1D integrable field theory in Ref. [26]. Precisely, off-diagonal matrix elements between eigenstates in the same macrostate decay exponentially with the chain size L , as in the standard *ETH* scenario for chaotic models (cf. (1)). Off-diagonal matrix elements between eigenstates in different macrostates decay faster (cf. (3)). Interestingly, integrability is reflected in the statistics of the matrix elements, which is encoded in the distribution of the R_{ij} in (1). In the standard *ETH* scenario, R_{ij} follow a Gaussian distribution with zero mean. On the other hand, we showed that for the *XXX* chain the distribution is well described by a Gumbel distribution.

Our work opens several new directions for future investigations. For instance, it would be interesting to employ our method to investigate the relationship between the statistics of off-diagonal matrix elements and Free Probability Theory (*FPT*). The most urging question is to what extent *FPT* results [5] also apply to integrable

models. Second, it was shown recently that the *ETH* scenario, complemented with the *FPT*, can be applied to describe the statistics of the overlaps between pre-quench initial states and eigenstates of chaotic systems [44]. It would be interesting to check this scenario. This is accessible by combining our method with the results of Ref. [43]. Finally, from the statistics of the matrix elements and the overlaps it is possible, in principle, to reconstruct the full-time dynamics of observables. This direction was investigated for the Lieb-Liniger model in Ref. [45]. It would be interesting to extend this results to lattice integrable systems. This would also allow to investigate relaxation dynamics and its relationship with *ETH* [46–50].

ACKNOWLEDGMENTS

We would like to thank Fabian Essler for useful discussions. We also thank the *GGI* Florence for hospitality during the “SFT 2025 - Lectures on Statistical Field Theories”, during which part of this work was done. This study was carried out within the National Centre on HPC, Big Data and Quantum Computing - SPOKE 10 (Quantum Computing) and received funding from the European Union Next-GenerationEU - National Recovery and Resilience Plan (NRRP) – MISSION 4 COMPONENT 2, INVESTMENT N. 1.4 – CUP N. I53C22000690001. This work has been supported by the project “Artificially devised many-body quantum dynamics in low dimensions - ManyQLowD” funded by the MIUR Progetti di Ricerca di Rilevante Interesse Nazionale (PRIN) Bando 2022 - grant 2022R35ZBF.

-
- [1] J. M. Deutsch, Quantum statistical mechanics in a closed system, *Phys. Rev. A* **43**, 2046 (1991).
 - [2] M. Srednicki, Chaos and Quantum Thermalization, *Phys. Rev. E* **50**, 888 (1994), [arXiv:cond-mat/9403051](#).
 - [3] M. Srednicki, The approach to thermal equilibrium in quantized chaotic systems, *J. Phys. A* **32**, 1163 (1999), [arXiv:cond-mat/9809360](#).
 - [4] L. D’Alessio, Y. Kafri, A. Polkovnikov, and M. R. and, From quantum chaos and eigenstate thermalization to statistical mechanics and thermodynamics, *Advances in Physics* **65**, 239 (2016), <https://doi.org/10.1080/00018732.2016.1198134>.
 - [5] S. Pappalardi, L. Foini, and J. Kurchan, Eigenstate Thermalization Hypothesis and Free Probability, *Phys. Rev. Lett.* **129**, 170603 (2022).
 - [6] D. Bernard and L. Hruza, Exact entanglement in the driven quantum symmetric simple exclusion process, *SciPost Phys.* **15**, 175 (2023).
 - [7] M. Rigol, V. Dunjko, and M. Olshanii, Thermalization and its mechanism for generic isolated quantum systems, *Nature* **452**, 854 (2008).
 - [8] R. Steinigeweg, J. Herbrych, and P. Prelovšek, Eigenstate thermalization within isolated spin-chain systems, *Phys. Rev. E* **87**, 012118 (2013).
 - [9] W. Beugeling, R. Moessner, and M. Haque, Off-diagonal matrix elements of local operators in many-body quantum systems, *Phys. Rev. E* **91**, 012144 (2015).
 - [10] A. Chandran, M. D. Schulz, and F. J. Burnell, The eigenstate thermalization hypothesis in constrained Hilbert spaces: A case study in non-Abelian anyon chains, *Phys. Rev. B* **94**, 235122 (2016).

- [11] R. Mondaini and M. Rigol, Eigenstate thermalization in the two-dimensional transverse field Ising model. II. Off-diagonal matrix elements of observables, *Phys. Rev. E* **96**, 012157 (2017).
- [12] C. Nation and D. Porras, Off-diagonal observable elements from random matrix theory: distributions, fluctuations, and eigenstate thermalization, *New Journal of Physics* **20**, 103003 (2018).
- [13] T. Yoshizawa, E. Iyoda, and T. Sagawa, Numerical Large Deviation Analysis of the Eigenstate Thermalization Hypothesis, *Phys. Rev. Lett.* **120**, 200604 (2018).
- [14] M. Rigol and L. F. Santos, Quantum chaos and thermalization in gapped systems, *Phys. Rev. A* **82**, 011604 (2010).
- [15] G. Biroli, C. Kollath, and A. M. Läuchli, Effect of Rare Fluctuations on the Thermalization of Isolated Quantum Systems, *Phys. Rev. Lett.* **105**, 250401 (2010).
- [16] E. Khatami, G. Pupillo, M. Srednicki, and M. Rigol, Fluctuation-Dissipation Theorem in an Isolated System of Quantum Dipolar Bosons after a Quench, *Phys. Rev. Lett.* **111**, 050403 (2013).
- [17] T. LeBlond, K. Mallayya, L. Vidmar, and M. Rigol, Entanglement and matrix elements of observables in interacting integrable systems, *Phys. Rev. E* **100**, 062134 (2019).
- [18] M. Brenes, J. Goold, and M. Rigol, Low-frequency behavior of off-diagonal matrix elements in the integrable XXZ chain and in a locally perturbed quantum-chaotic XXZ chain, *Phys. Rev. B* **102**, 075127 (2020).
- [19] T. LeBlond and M. Rigol, Eigenstate thermalization for observables that break Hamiltonian symmetries and its counterpart in interacting integrable systems, *Phys. Rev. E* **102**, 062113 (2020).
- [20] M. Mierzejewski and L. Vidmar, Quantitative Impact of Integrals of Motion on the Eigenstate Thermalization Hypothesis, *Phys. Rev. Lett.* **124**, 040603 (2020).
- [21] Y. Zhang, L. Vidmar, and M. Rigol, Statistical properties of the off-diagonal matrix elements of observables in eigenstates of integrable systems, *Phys. Rev. E* **106**, 014132 (2022).
- [22] R. Patil and M. Rigol, Eigenstate thermalization in spin-1/2 systems with SU(2) symmetry (2025), [arXiv:2503.01846 \[quant-ph\]](#).
- [23] T. N. Ikeda, Y. Watanabe, and M. Ueda, Finite-size scaling analysis of the eigenstate thermalization hypothesis in a one-dimensional interacting Bose gas, *Phys. Rev. E* **87**, 012125 (2013).
- [24] V. Alba, M. Fagotti, and P. Calabrese, Entanglement entropy of excited states, *J. Stat. Mech.* **0910**, P10020 (2009), [arXiv:0909.1999](#).
- [25] V. Alba, Eigenstate thermalization hypothesis and integrability in quantum spin chains, *Phys. Rev. B* **91**, 155123 (2015), [arXiv:1409.6096](#).
- [26] F. H. L. Essler and A. J. J. M. de Klerk, Statistics of Matrix Elements of Local Operators in Integrable Models, *Phys. Rev. X* **14**, 031048 (2024), [arXiv:2307.12410](#).
- [27] J.-S. Caux, P. Calabrese, and N. A. Slavnov, One-particle dynamical correlations in the one-dimensional Bose gas, *Journal of Statistical Mechanics: Theory and Experiment* **2007**, P01008 (2007).
- [28] L. Piroli and P. Calabrese, Exact formulas for the form factors of local operators in the Lieb–Liniger model, *Journal of Physics A: Mathematical and Theoretical* **48**, 454002 (2015).
- [29] M. Horvath, A. Bastianello, S. Dhar, R. Koch, Y. Guo, J.-S. Caux, M. Landini, and H.-C. Nägerl, Observing Bethe strings in an attractive Bose gas far from equilibrium (2025), [arXiv:2505.10550 \[cond-mat.quant-gas\]](#).
- [30] N. Kitanine, J. M. Maillet, and V. Terras, Form factors of the XXZ Heisenberg spin- $\frac{1}{2}$ finite chain, *Nucl. Phys. B* **554**, 647 (1999), [arXiv:math-ph/9807020](#).
- [31] N. Kitanine, J. M. Maillet, and V. Terras, Correlation functions of the XXZ Heisenberg spin- $\frac{1}{2}$ chain in a magnetic field, *Nucl. Phys. B* **567**, 554 (2000), [arXiv:math-ph/9907019](#).
- [32] J.-S. Caux and J. M. Maillet, Computation of Dynamical Correlation Functions of Heisenberg Chains in a Magnetic Field, *Phys. Rev. Lett.* **95**, 077201 (2005).
- [33] J.-S. Caux, R. Hagemans, and J. M. Maillet, Computation of dynamical correlation functions of Heisenberg chains: the gapless anisotropic regime, *Journal of Statistical Mechanics: Theory and Experiment* **2005**, P09003 (2005).
- [34] J.-S. Caux and P. Calabrese, Dynamical density-density correlations in the one-dimensional Bose gas, *Phys. Rev. A* **74**, 031605 (2006).
- [35] J.-S. Caux, Correlation functions of integrable models: A description of the ABACUS algorithm, *Journal of Mathematical Physics* **50**, 095214 (2009).
- [36] M. Takahashi, *Thermodynamics of One-Dimensional Solvable Models* (Cambridge University Press, 1999).
- [37] H. Bethe, Zur Theorie der Metalle, *Zeitschrift für Physik* **71**, 205 (1931).
- [38] V. E. Korepin, N. M. Bogoliubov, and A. G. Izergin, *Quantum Inverse Scattering Method and Correlation Functions*, Cambridge Monographs on Mathematical Physics (Cambridge University Press, 1993).
- [39] F. H. L. Essler, H. Frahm, F. Göhmann, A. Klümper, and V. E. Korepin, *The One-Dimensional Hubbard Model* (Cambridge University Press, 2005).
- [40] R. Hagemans and J.-S. Caux, Deformed strings in the Heisenberg model, *Journal of Physics A: Mathematical and Theoretical* **40**, 14605 (2007).
- [41] P. Calabrese, F. H. L. Essler, and G. Mussardo, Introduction to ‘Quantum Integrability in Out of Equilibrium Systems’, *Journal of Statistical Mechanics: Theory and Experiment* **2016**, 064001 (2016).

- [42] V. Alba, *Simulating the Generalized Gibbs Ensemble (GGE): a Hilbert space Monte Carlo approach* (2015), [arXiv:1507.06994 \[cond-mat.str-el\]](#).
- [43] V. Alba and P. Calabrese, The quench action approach in finite integrable spin chains, *Journal of Statistical Mechanics: Theory and Experiment* **2016**, 043105 (2016).
- [44] L. Foini, A. Dymarsky, and S. Pappalardi, Out-of-equilibrium eigenstate thermalization hypothesis, *SciPost Phys.* **18**, 136 (2025).
- [45] J. D. Nardis, L. Piroli, and J.-S. Caux, Relaxation dynamics of local observables in integrable systems, *Journal of Physics A: Mathematical and Theoretical* **48**, 43FT01 (2015).
- [46] I. A. Maceira and A. M. Läuchli, *Thermalization Dynamics in Closed Quantum Many Body Systems: a Precision Large Scale Exact Diagonalization Study* (2024), [arXiv:2409.18863 \[quant-ph\]](#).
- [47] J. Wang, R. Mishra, T.-H. Yang, L. V. Delacrétaz, and S. Pappalardi, *Eigenstate Thermalization Hypothesis correlations via non-linear Hydrodynamics* (2025), [arXiv:2505.06869 \[cond-mat.stat-mech\]](#).
- [48] F. Fritzsche, T. Prosen, and S. Pappalardi, Micro-canonical free cumulants in lattice systems, *Phys. Rev. B* **111**, 054303 (2025).
- [49] O. Bouverot-Dupuis, S. Pappalardi, J. Kurchan, A. Polkovnikov, and L. Foini, *Random matrix universality in dynamical correlation functions at late times* (2025), [arXiv:2407.12103 \[cond-mat.stat-mech\]](#).
- [50] L. Capizzi, J. Wang, X. Xu, L. Mazza, and D. Poletti, Hydrodynamics and the Eigenstate Thermalization Hypothesis, *Phys. Rev. X* **15**, 011059 (2025).
- [51] N. A. Slavnov, Calculation of scalar products of wave functions and form factors in the framework of the algebraic Bethe ansatz, *Theor. Math. Phys.* **79**, 502 (1989).

Appendix A: Matrix elements of local operators in the XXZ chain

In this appendix, we review the exact result of Refs. [30, 31] for the matrix elements of the elementary operators (16) between energy eigenstates of the XXZ spin-1/2 chain. The Hamiltonian of the model is

$$H = \frac{1}{4} \sum_{i=1}^L \frac{1}{2} (\sigma_i^+ \sigma_{i+1}^- + \sigma_i^- \sigma_{i+1}^+) + \Delta \sigma_i^z \sigma_{i+1}^z, \quad (\text{A1})$$

where, as in the main text, $\vec{\sigma}_i$ are the Pauli matrices and the chain has length L . The parameter Δ is the anisotropy of the spin-spin interaction and, in the isotropic limit $\Delta = 1$, the model (A1) reduces to the XXX spin chain (5) studied in the main text. The Hamiltonian (A1) has a global $U(1)$ symmetry corresponding to the conservation of the total magnetization $S^z = 1/2 \sum_{i=1}^L \sigma_i^z$. As mentioned in the main text, at $\Delta = 1$ this symmetry is enhanced to the full $SU(2)$ group of global spin rotations. In the following, in order to treat both the case $\Delta = 1$ and $0 < \Delta < 1$ in a unified way, we define

$$\phi(\lambda) = \begin{cases} \lambda, & \Delta = 1, \\ \sinh \lambda, & 0 < \Delta < 1, \end{cases} \quad (\text{A2})$$

$$\eta = \begin{cases} -i, & \Delta = 1, \\ -\operatorname{arccosh} \Delta, & 0 < \Delta < 1. \end{cases} \quad (\text{A3})$$

To obtain the energy spectrum of the Hamiltonian (A1) and to compute matrix elements of operators we will use the ABA formalism [38]. In this formalism, for each site, one introduces an R -matrix, which for the XXZ chain takes the form

$$R_{0i}(\lambda - \xi) = \begin{pmatrix} 1 & 0 & 0 & 0 \\ 0 & \frac{\phi(\lambda - \xi)}{\phi(\lambda - \xi + \eta)} & 0 & 0 \\ 0 & 0 & \frac{\phi(\eta)}{\phi(\lambda - \xi + \eta)} & 0 \\ 0 & 0 & 0 & 1 \end{pmatrix}. \quad (\text{A4})$$

The R -matrix (A4) acts on the tensor product of the Hilbert space \mathcal{H}_i of the i -th site and on an auxiliary space \mathcal{H}_0 isomorphic to \mathbb{C}^2 . The so-called monodromy matrix T is then defined as the product in the auxiliary space of the R -matrices in each site as

$$\begin{aligned} T(\lambda; \{\xi_i\}) &= R_{0N}(\lambda - \xi_N) \dots R_{01}(\lambda - \xi_1) \\ &= \begin{pmatrix} A(\lambda; \{\xi_i\}) & B(\lambda; \{\xi_i\}) \\ C(\lambda; \{\xi_i\}) & D(\lambda; \{\xi_i\}) \end{pmatrix}, \end{aligned} \quad (\text{A5})$$

where the matrix T acts on the product of the auxiliary $\mathcal{H}_0 \simeq \mathbb{C}^2$ space and the Hilbert space

$\mathcal{H} = \bigotimes_{i=1}^L \mathcal{H}_i$ of the whole chain, while A, B, C and D are operators acting only on \mathcal{H} . Following Refs. [30, 31], we have furthermore introduced arbitrary inhomogeneities $\{\xi_i\}$, $i = 1, \dots, L$ sitting at each site i .

The monodromy matrix (A5) allows us to construct the Fock space of the model. Starting from the pseudovacuum state $|0\rangle$, which for the XXZ chain is the ferromagnetic state with all spins up $|0\rangle = |\uparrow\uparrow\uparrow\dots\rangle$, the matrices $B(\mu)$ and $C(\mu)$ in Eq. (A5) act on the pseudovacuum $|0\rangle$ respectively as creation and annihilation operators of particles with rapidities μ_i

$$|\{\mu\}\rangle = \prod_{k=1}^M B(\mu_k) |0\rangle, \quad \langle\{\mu\}| = \langle 0| \prod_{k=1}^M C(\mu_k). \quad (\text{A6})$$

We remark that not all particle states (A6) are eigenstates of the Hamiltonian (A1) and, as a consequence, they are not all orthogonal to each other, forming an overcomplete basis. To find the eigenstates of Eq. (A1), we define the transfer matrix \mathcal{T} as the trace over the internal space of the monodromy matrix (A5) $\mathcal{T}(\lambda) = \text{Tr} T(\lambda; \{\xi_i\}) = A(\lambda; \{\xi_i\}) + D(\lambda; \{\xi_i\})$. The transfer matrix evaluated at two generic rapidities λ, μ commute with each other $[\mathcal{T}(\lambda), \mathcal{T}(\mu)] = 0$, meaning that they can be diagonalized simultaneously. Since λ, μ are arbitrary, this implies that we can diagonalize $\mathcal{T}(\lambda)$.

Moreover, in the homogeneous limit $\forall i, \xi_i \rightarrow \eta/2$, the eigenstates of \mathcal{T} are also eigenstates of the XXZ Hamiltonian (A1). Applying the transfer matrix to the states (A6), one obtains that the rapidities of the Hamiltonian eigenstates must satisfy a set of non-linear equations known as Bethe equations. In the presence of the inhomogeneities ξ_i the Bethe equations take the form

$$d(\lambda_i) \prod_{j \neq i} \frac{\phi(\lambda_j - \lambda_i - \eta)}{\phi(\lambda_j - \lambda_i + \eta)} = 1, \quad (\text{A7})$$

where the function $d(\lambda)$ is defined as

$$d(\lambda) = \prod_{i=1}^L \frac{\phi(\lambda - \xi_i)}{\phi(\lambda - \xi_i + \eta)}. \quad (\text{A8})$$

Notice in particular that Eq. (A8) vanishes when computed on the inhomogeneities, i.e., $d(\xi_i) = 0$. The results for the XXZ chain are obtained by taking the homogeneous limit $\xi_i \rightarrow \eta/2$. Importantly, the homogeneous limit is plagued by fictitious singularities that have to be removed to recover physical results.

Moreover, as discussed already in Section II, the Bethe equations (A7) admit solutions containing both real and complex rapidities. Solving the Bethe equations for generic complex rapidities is a daunting task. However, according to the string hypothesis [36], in the thermodynamic limit $L \rightarrow \infty$, the vast majority of complex solutions organizes in groups of n rapidities known as Bethe string, which have identical real part and imaginary parts equally spaced by η . Physically, these strings states correspond to bound states of n excitations moving collectively. In practice, at finite L the string hypothesis is valid only approximately, and the rapidities in the same string exhibit deviations δ which are exponentially small in L . Assuming that the string hypothesis holds exactly even at finite (large) L allows one to simplify considerably the solution of Eq. (A7). By taking the limit of zero string deviations $\delta \rightarrow 0$ in (A7), one obtains the Bethe-Gaudin-Takahashi equations (9) for the real parts of the strings. Again, the limit $\delta \rightarrow 0$ introduces additional fictitious singularities in the ABA formulas for the matrix elements.

1. Scalar product of Bethe states

A crucial ingredient in the ABA formulas for the matrix elements of local operators is the so-called Slavnov formula for scalar products between Bethe states [38]. Let $|\{\lambda\}\rangle$ be a Bethe state, with M rapidities satisfying the Bethe equations (A7), and let $|\{\mu\}\rangle$ be a state of the form (A6) with M arbitrary parameters μ . Clearly, the state $|\{\mu\}\rangle$ for generic $\{\mu\}$ is not an eigenstate of the XXZ chain. The two states are generically not orthogonal and their scalar product is given by the Slavnov formula [38, 51]

$$\langle\{\mu\}|\{\lambda\}\rangle = \frac{\det \mathbf{S}}{\prod_{i=1}^M \prod_{j < i} \phi(\mu_i - \mu_j) \phi(\lambda_j - \lambda_i)}, \quad (\text{A9})$$

where \mathbf{S} is the Slavnov matrix [38, 51]

$$\mathbf{S}_{ab} = -G_b^+ [K_{ab}^+ - K_{ab}^- R_b], \quad (\text{A10})$$

and we have introduced

$$K_{ab}^\pm = \frac{\phi(\eta)}{\phi(\lambda_a - \mu_b) \phi(\lambda_a - \mu_b \pm \eta)}, \quad (\text{A11})$$

$$G_b^\pm = \prod_{i=1}^M \phi(\lambda_i - \mu_b \pm \eta), \quad (\text{A12})$$

$$R_b = d(\mu_b) \prod_{i=1}^M \frac{\phi(\lambda_i - \mu_b - \eta)}{\phi(\lambda_i - \mu_b + \eta)} = \frac{G_b^-}{G_b^+} d(\mu_b). \quad (\text{A13})$$

If $\{\mu\}$ are also solutions of the Bethe equations, $|\{\mu\}\rangle$ is an eigenstate of the XXZ chain, and we can use the Bethe equation (A7) to replace $d(\mu_b) = \prod_{i \neq b} \phi(\mu_i - \mu_b + \eta) / \phi(\mu_i - \mu_b - \eta)$ in the Slavnov matrix (A10). As a consequence now R_b becomes

$$R_b = -\frac{G_b^- \tilde{F}_b^+}{G_b^+ \tilde{F}_b^-}, \quad (\text{A14})$$

where we have defined

$$\tilde{F}_b^\pm = \prod_{i=1}^M \phi(\mu_i - \mu_b \pm \eta). \quad (\text{A15})$$

While the previous expressions are always well defined for states with only real rapidities, for Bethe strings Eq. (A15) vanishes. The rows of the Slavnov matrix (A10) are then singular, although the determinant should remain finite. For simplicity, let us assume that $\{\mu\}$ contain only a single n -string, and let us rearrange $\{\mu\}$ such that the first n rapidities are the ones forming the n -string. Following [32], we introduce string deviations δ for the first n rapidities $\{\mu\}$. Then, we sum the first n rows of the matrix (A10). This operation remove the singularities without changing the determinant, allowing us to take the limit $\delta \rightarrow 0$. After these manipulations, the columns corresponding to the n strings in the Slavnov matrix Eq. (A10) are modified as

$$\mathbf{S}'_{ab} = \begin{cases} -G_b^+ K_{ab}^+, & b < n, \\ -G_n^+ \left[K_{an}^+ - K_{a1}^- \prod_{i=1}^n R_i + \right. \\ \quad \left. - \sum_{j=2}^n \left(\partial K_{aj}^+ \prod_{i=j}^n R_i \right) \right], & b = n, \end{cases} \quad (\text{A16})$$

where $b = 1, 2, \dots, n$, and the derivative of the expression K_{ab}^+ is

$$\partial K_{ab}^+ = -\frac{\phi(\eta) \phi(2\lambda - \eta)}{\phi(\lambda)^2 \phi(\lambda - \eta)^2}. \quad (\text{A17})$$

The remaining columns of Eq. (A10) are unchanged. Notice that in the case $n = 1$, i.e., for a real rapidity, Eq. (A16) reduces to Eq. (A10), as expected. The procedure outlined above is straightforwardly generalized to the case in which $\{\mu\}$ contain an arbitrary

number of strings [32] because different strings can be treated independently.

Let us now discuss the norm of the Bethe states. The norm is obtained from the Slavnov formula (A9) by taking the limit $\{\mu\} \rightarrow \{\lambda\}$ in the matrix (A10). One obtains the so-called Gaudin formula [38]

$$\langle \{\lambda\} | \{\lambda\} \rangle = \frac{\det \mathbf{G}}{\prod_{i=1}^M \prod_{j \neq i} \phi(\lambda_i - \lambda_j)}, \quad (\text{A18})$$

where the elements of the Gaudin matrix \mathbf{G} are [38]

$$\mathbf{G}_{ab} = -G_b^+ \left[k^{(2)}(\lambda_a - \lambda_b) + \delta_{ab} \left(\frac{d'(\lambda_b)}{d(\lambda_b)} - \sum_{j=1}^M k^{(2)}(\lambda_j - \lambda_b) \right) \right], \quad (\text{A19})$$

and we have introduced the notation

$$k^{(2)}(\lambda) = \frac{\phi(2\eta)}{\phi(\lambda + \eta) \phi(\lambda - \eta)}. \quad (\text{A20})$$

Similar to the Slavnov matrix, the Gaudin matrix is singular if strings are present. The strategy employed to remove the singularities in the Slavnov matrix has to be modified because the limit $\{\mu\} \rightarrow \{\lambda\}$ and the limit $\delta \rightarrow 0$ do not commute. We introduce F_b^\pm to be the finite part of \tilde{F}_b^\pm obtained by isolating the singular part in the limit $\delta \rightarrow 0$

$$F_b^+ \approx \begin{cases} (\delta_b - \delta_{b+1})^{-1} \tilde{F}_b^+, & b < n, \\ \tilde{F}_b^+, & b = n. \end{cases} \quad (\text{A21})$$

$$F_b^- \approx \begin{cases} (\delta_{b-1} - \delta_b)^{-1} \tilde{F}_b^-, & 1 < b \leq n, \\ \tilde{F}_b^-, & b = 1. \end{cases} \quad (\text{A22})$$

where δ_b is the deviation of the rapidity λ_b . We obtain that the columns in the Gaudin matrix that correspond to a n -string are modified as

$$\mathbf{G}'_{ab} = \begin{cases} F_b^+, & a = b, \\ -F_b^+, & a = b + 1, \\ 0, & \text{otherwise,} \end{cases} \quad b < n, \quad (\text{A23})$$

$$\mathbf{G}'_{an} = \begin{cases} -F_n^+ \left(\frac{d'(\lambda_a)}{d(\lambda_a)} + \right. \\ \quad \left. - \sum_{j>n} k^{(2)}(\lambda_a - \lambda_j) \right), & a \leq n, \\ -F_n^+ \sum_{j \leq n} k^{(2)}(\lambda_a - \lambda_j), & a > n, \end{cases}$$

where the sum over $j > n$ in \mathbf{G}'_{an} is carried over all the rapidities that do not belong to the string, including possibly all other strings. Again we see that for $n = 1$, Eq. (A23) reduces to Eq. (A19).

2. Matrix elements of local operators

We now provide the formulas for matrix elements of local operators between eigenstates of the XXZ chain. In Section A 2 a we provide the general formula for operators having nontrivial support on ℓ consecutive sites. In Section A 2 b we discuss the case with $\ell = 1$, providing the result also for eigenstates that contain Bethe strings.

a. General formulas for ℓ -spin operators

In the main text we studied operators constructed from elementary ones $E_j^{(\alpha,\beta)}$ acting on a generic site i of the chain as

$$\begin{aligned} E_i^{(11)} &= \frac{1}{2}(\mathbb{1}_i + \sigma_i^z), & E_i^{(12)} &= \frac{1}{2}(\sigma_i^x + i\sigma_i^y), \\ E_i^{(21)} &= \frac{1}{2}(\sigma_i^x - i\sigma_i^y), & E_i^{(22)} &= \frac{1}{2}(\mathbb{1}_i - \sigma_i^z). \end{aligned} \quad (\text{A24})$$

In Refs. [30, 31], the authors demonstrated that the local operators (A24) can be written in terms of the monodromy matrix T (A5) and the transfer matrix

$\mathcal{T} = A + D$ as

$$E_i^{(\epsilon_i, \epsilon'_i)} = \left(\prod_{j < i} \mathcal{T}(\xi_j) \right) T_{\epsilon_i, \epsilon'_i}(\xi_i) \left(\prod_{j > i} \mathcal{T}(\xi_j) \right). \quad (\text{A25})$$

One can exploit the fact that the Bethe state $|\{\lambda\}\rangle$ is an eigenstate of the transfer matrix \mathcal{T} . Indeed, by using Eq. (A25) and by applying the transfer matrix to the right eigenstate, we can write

$$\langle \{\mu\} | \prod_{i=1}^{\ell} E_i^{(\epsilon_i, \epsilon'_i)} | \{\lambda\} \rangle = \Phi_{\ell}(\{\lambda\}) \langle \{\mu\} | \prod_{i=1}^{\ell} T_{\epsilon_i, \epsilon'_i} | \{\lambda\} \rangle, \quad (\text{A26})$$

where

$$\Phi_{\ell}(\{\lambda\}) = \prod_{j=1}^{\ell} \prod_{a=1}^M \frac{\phi(\lambda_a - \xi_j)}{\phi(\lambda_a - \xi_j + \eta)}, \quad (\text{A27})$$

is the product of the eigenvalues of $\mathcal{T}(\xi_j)$. To compute the matrix element we then apply the operators A, B, C and D in Eq. (A5) on the state $\langle \{\mu\} |$ on the left. Recalling the definition (A6) for the state $\langle \{\mu\} |$, we observe that $C(\mu_{M+1})$ acts as a creation operator for an additional excitation with rapidity μ_{M+1} . However, the action of A, B and D is more complicated and it is given as [24, 30, 31]

$$\langle 0 | \prod_{k=1}^M C(\mu_k) A(\mu_{M+1}) = \sum_{a'=1}^{M+1} \frac{\prod_{k=1}^M \phi(\mu_k - \mu_{a'} + \eta)}{\prod_{k=1, k \neq a'}^{M+1} \phi(\mu_k - \mu_{a'})} \left(\langle 0 | \prod_{k=1, k \neq a'}^{M+1} C(\mu_k) \right), \quad (\text{A28})$$

$$\langle 0 | \prod_{k=1}^M C(\mu_k) D(\mu_{M+1}) = \sum_{a=1}^{M+1} d(\mu_a) \frac{\prod_{k=1}^M \phi(\mu_k - \mu_a - \eta)}{\prod_{k=1, k \neq a}^{M+1} \phi(\mu_k - \mu_a)} \left(\langle 0 | \prod_{k=1, k \neq a}^{M+1} C(\mu_k) \right), \quad (\text{A29})$$

$$\begin{aligned} \langle 0 | \prod_{k=1}^M C(\mu_k) B(\mu_{M+1}) &= \sum_{a=1}^M d(\mu_a) \frac{\prod_{k=1}^M \phi(\mu_k - \mu_a - \eta)}{\prod_{k=1, k \neq a}^{M+1} \phi(\mu_k - \mu_a)} \times \\ &\times \sum_{a'=1, a' \neq a}^{M+1} \frac{\prod_{k=1, k \neq a}^M \phi(\mu_k - \mu_{a'} - \eta)}{\prod_{k=1, k \neq a, a'}^{M+1} \phi(\mu_k - \mu_{a'})} \left(\langle 0 | \prod_{k=1, k \neq a, a'}^{M+1} C(\mu_k) \right). \end{aligned} \quad (\text{A30})$$

In Eq. (A30), we used the fact that in the case of interest $\mu_{M+1} = \xi$ and $d(\xi) = 0$ to simplify the expression [24, 30, 31]. By recursively applying the outlined expressions, we obtain the action of a string of local operators on any Bethe state. To express the result in a closed form, we define the two set of

indices α^{\pm} as [24, 30, 31]

$$\begin{aligned} \alpha^+ &= \{j : 1 \leq j \leq \ell, \epsilon_j = +\}, \\ \alpha^- &= \{j : 1 \leq j \leq \ell, \epsilon'_j = -\}. \end{aligned} \quad (\text{A31})$$

For every index $j \in \alpha^+$ ($j \in \alpha^-$), we furthermore introduce a set a_j (a'_j) such that

$$\begin{aligned} 1 \leq a_j \leq M + j, a_j \in \mathbf{A}_j \text{ for } j \in \alpha^-, \\ 1 \leq a'_j \leq M + j, a'_j \in \mathbf{A}'_j \text{ for } j \in \alpha^+, \end{aligned} \quad (\text{A32})$$

where the sets \mathbf{A}_j and \mathbf{A}'_j are recursively defined as

$$\begin{aligned} \mathbf{A}_j &= \{b \in [1, M + \ell] : b \neq a_k, a'_k \text{ with } k < j\}, \\ \mathbf{A}'_j &= \{b \in [1, M + \ell] : b \neq a_k \text{ with } k < j, \\ &\quad \text{and } b \neq a'_k \text{ with } k \leq j\}. \end{aligned} \quad (\text{A33})$$

With these definitions, we can finally write

$$\begin{aligned} \langle 0 | \prod_{k=1}^M C(\mu_k) \prod_{j=1}^{\ell} T_{\epsilon_j \epsilon_{j'}}(\mu_{M+j}) \\ = \sum_{\{a_j, a'_j\}} G_{\{a_j, a'_j\}}(\mu) \left(\langle 0 | \prod_{b \in \mathbf{A}_{s+1}} C(\mu_b) \right), \end{aligned} \quad (\text{A34})$$

where we defined

$$\begin{aligned} G_{\{a_j, a'_j\}} &= \prod_{j \in \alpha^-} d(\mu_{a_j}) \frac{\prod_{b=1, b \in \mathbf{A}_j}^{M+j-1} \phi(\mu_b - \mu_{a_j} - \eta)}{\prod_{b=1, b \in \mathbf{A}'_j}^{M+j} \phi(\mu_b - \mu_{a_j})} \times \\ &\times \prod_{j \in \alpha^+} \frac{\prod_{b=1, b \in \mathbf{A}'_j}^{M+j-1} \phi(\mu_b - \mu_{a'_j} + \eta)}{\prod_{b=1, b \in \mathbf{A}_{j+1}}^{M+j} \phi(\mu_b - \mu_{a'_j})}. \end{aligned} \quad (\text{A35})$$

in terms of the sets \mathbf{A}_j and \mathbf{A}'_j .

Finally in order to obtain the matrix elements we take the homogeneous limit $\xi_j \rightarrow \eta/2$. As explained in Ref. [24], however, this introduces singularities due to the terms that contain the operators A and B . Moreover, for most of the matrix elements, besides multiplicative singularities, there remain additional poles which cancel out between the different terms in the sum [24]. For states which only include real rapidities, the procedure to remove the singularities was discussed in Ref. [24]. However, in the presence of strings, the limit of vanishing string deviations and the inhomogeneous limit do not commute, and an efficient procedure to obtain the matrix elements between generic eigenstates of the XXZ chain also in the presence of strings is not available yet. A notable exception is the case of one-spin operator, i.e., $\ell = 1$, which we discuss in Section A 2 b.

b. One-spin operators

For operators acting on a single spin the inhomogeneous limit does not introduce any singularity.

Thus, the limit $\delta \rightarrow 0$, i.e., of vanishing string deviations can be performed efficiently. Moreover, by using properties of rank-1 matrices, the matrix element of one-spin operators can be expressed as a single determinant, instead of a sum of multiple determinants. Precisely, we can use that if P is a rank-1 matrix and M is a generic one, the determinant of their sum is

$$\det(M + P) = \det M + \sum_{j=1}^M \det M^{(j)}, \quad (\text{A36})$$

where $M^{(j)}$ is the matrix obtained by replacing the j -th column of M with the j -th column of P .

From Eq. (A28) we observe that the matrix elements of $E_i^{(11)}$, which are proportional to the matrix elements of A , are written as sum of determinants as in (A36). Each term in the sum is the determinant of a matrix that is obtained from the Slavnov matrix (A9) (or the Gaudin matrix (A19) for diagonal matrix elements) by replacing a single column with a column of the matrix P defined as [31]

$$\begin{aligned} \mathbf{P}_{ab} &= \frac{\phi(\eta) \prod_{i=1}^M \phi(\mu_i - \mu_b + \eta)}{\phi(\lambda_a - \frac{\eta}{2}) \phi(\lambda_a + \frac{\eta}{2})} \\ &= \frac{\phi(\eta) F_b^+}{\phi(\lambda_a - \frac{\eta}{2}) \phi(\lambda_a + \frac{\eta}{2})}. \end{aligned} \quad (\text{A37})$$

By using Eq. (A36), one obtains that the off-diagonal matrix elements of one-spin operators can then be written as

$$\begin{aligned} \langle \{\mu\} | E^{(11)} | \{\lambda\} \rangle &= \frac{\prod_{i=1}^M \phi(\lambda_i + \frac{\eta}{2})}{\prod_{i=1}^M \phi(\mu_i + \frac{\eta}{2})} \\ &\times \frac{\det(\mathbf{S} + \mathbf{P})}{\prod_{i=1}^M \prod_{j < i} \phi(\lambda_i - \lambda_j) \phi(\mu_j - \mu_i)}, \end{aligned} \quad (\text{A38})$$

where \mathbf{S} is the Slavnov matrix. The diagonal matrix elements can be obtained by simply substituting the Slavnov matrix \mathbf{S} with the Gaudin matrix \mathbf{G} . By using this result and the relation $E^{(22)} = \mathbf{1} - E^{(11)}$, we also obtain $\langle \{\mu\} | E^{(11)} | \{\lambda\} \rangle = \langle \{\mu\} | \{\lambda\} \rangle - \langle \{\mu\} | E^{(22)} | \{\lambda\} \rangle$.

Having the matrix elements in the form (A38), it is now possible to treat eigenstates containing strings. Indeed, in the presence of an n -string $\{\mu_1, \dots, \mu_n\}$, the Slavnov matrix \mathbf{S} can be modified as in Eq. (A16), by recursively adding the columns of the block corresponding to the string. In order to preserve the determinant, the same operations

have to be performed on the matrix \mathbf{P} , yielding

$$\mathbf{P}'_{ab} = \begin{cases} 0, & b < n, \\ \frac{\phi(\eta) G_n^+}{\phi(\lambda_a - \frac{\eta}{2}) \phi(\lambda_a + \frac{\eta}{2})} \times \\ \quad \times \sum_{j=1}^n \frac{F_j^+}{G_j^+} \left(\prod_{i=j+1}^M R_i \right), & b = n. \end{cases} \quad (\text{A39})$$

Let us now discuss the matrix elements of $E_i^{(21)}$. Unlike $E_i^{(11)}$, $E_i^{(21)}$ connects eigenstates with different number of particles. Now, one can check that $E_i^{(21)}$ is proportional to the creation operator $C(\eta/2)$. This means that the matrix elements between states $|\{\mu_k\}\rangle, j = 1, \dots, M$ and $|\{\lambda_j\}\rangle, j = 1, \dots, M+1$

is simply given by the formula

$$\begin{aligned} \langle \{\mu\} | E^{(12)} | \{\lambda\} \rangle &= \frac{\Phi(\{\lambda\})}{\prod_{k=1}^M \phi(\mu_k - \eta/2)} \\ &\times \frac{\det \mathbf{S}'}{\prod_{1 \leq i < j \leq M+1} \phi(\lambda_i - \lambda_j) \prod_{1 \leq l < m \leq M} \phi(\mu_l - \mu_m)} \end{aligned} \quad (\text{A40})$$

where \mathbf{S}' coincides with the Slavnov matrix \mathbf{S} except for the $M+1$ -th column, which is given as

$$\mathbf{S}'_{ab} = \begin{cases} \mathbf{S}_{ab}, & b \leq M, \\ -\phi(\eta) \frac{\prod_{j=1}^{M+1} \phi(\lambda_j + \eta/2)}{\phi(\lambda_a - \eta/2) \phi(\lambda_a + \eta/2)}, & b = M+1. \end{cases} \quad (\text{A41})$$

The matrix elements of $E^{(21)}$ are then simply obtained using $E^{(21)} = E^{(12)\dagger}$.